

Quantum Logic Gates in Optical Lattices

Gavin K. Brennen⁽¹⁾, Carlton M. Caves⁽¹⁾, Poul S. Jessen⁽²⁾, and Ivan H. Deutsch⁽¹⁾

⁽¹⁾Center for Advanced Studies, Department of Physics and Astronomy

University of New Mexico, Albuquerque, NM 87131

⁽²⁾Optical Sciences Center, University of Arizona, Tucson, AZ 85721

Abstract: We propose a new system for implementing quantum logic gates: neutral atoms trapped in a very far-off-resonance optical lattice. Pairs of atoms are made to occupy the same well by varying the polarization of the trapping lasers, and then a near-resonant electric dipole is induced by an auxiliary laser. A controlled-NOT can be implemented by conditioning the target atomic resonance on a resolvable level shift induced by the control atom. Atoms interact only during logical operations, thereby suppressing decoherence.

PACS Number(s): 03.67.Lx, 32.80.Qk, 32.80.Lg, 32.80.Pj

Any computation is constrained by the physical laws governing the machine that carries out the operations. Conventional computers operate according to the laws of classical physics, but an entirely new class of computers is possible using physical components that are governed by the laws of quantum mechanics [1]. As a consequence of the superposition principle, such a quantum computer can perform a huge number of computations simultaneously, a phenomenon known as quantum parallelism. Certain problems that are algorithmically “hard” on a classical computer, an example being factorization of large integers into their prime factors, could be solved efficiently on a quantum computer [2].

At the heart of quantum computation is the entanglement of many two-state systems (qubits), which form the register of the quantum computer. The requirements for implementing a quantum computer seem to be almost contradictory. On the one hand, the qubits must be strongly coupled to one another and to an external field to produce the conditional-logic operations and resulting entanglement required for quantum computation. On the other hand, coupling to other external influences must be minimized because it leads to decoherence, which destroys the superpositions necessary for quantum parallelism. Quantum error correction [2-6] and fault-tolerant computation [7,8] promise to defeat the deleterious effects of decoherence, but only if the coupling to the environment is sufficiently weak.

Several physical realizations of quantum computation have been proposed. One of the most promising is based on storing each qubit in the electronic state of an ultra-cold trapped ion, as proposed by Cirac and Zoller [9]. Because of their charge, ions interact strongly via their mutual Coulomb repulsion, thus allowing unitary manipulation of the qubits' joint state to be achieved with lasers. Using trapped Be^+ , the NIST group was able to demonstrate a “controlled-NOT” (C-NOT) quantum logic gate [10]. Because of their charge, however, the ions interact strongly with the environment, giving rise to decoherence channels from technical noise sources, such as Johnson noise in the endcaps of the Paul trap. Moreover, the highly nonlinear interactions between qubits make scaling to many ions difficult [11]. Elements of quantum computation have also been implemented in standard NMR apparatuses [12] and in cavity QED [13], but both of these schemes are fundamentally difficult to scale to many qubits. Solid-state systems, such as quantum dots [15], have also been proposed for realizing quantum computation, but the strong interactions that exist in a condensed-matter environment make decoherence an especially difficult problem.

In contrast to ions, a dilute gas of neutral atoms couples very weakly to the environment. The main source of quantum decoherence is spontaneous emission if the atom is excited by an external field, but this can be negligible if all manipulations are performed rapidly compared to the photon scattering rate. The atoms interact predominantly via an electric

dipole-dipole potential. Though atom-atom interactions are usually weak for atoms in the electronic ground state (van der Waals), they can be made strong through excitation of a near-resonant dipole. Since these dipoles can be turned “on” and “off” at will, atoms can be made to interact only during the conditional logic operations and not during single qubit manipulations or during periods of free evolution, thereby suppressing the coupling to the decohering environment.

As mentioned above, this scheme requires that the operations be performed in a time short compared to the photon scattering time. To see that this is possible, consider the following scaling argument. The photon scattering rate is $\Gamma' = s\Gamma/2$, where s is the saturation parameter proportional to the excited state population, and $\Gamma \sim k^3 |d_{eg}|^2 / \hbar$ is the spontaneous emission rate, k being the wave number of the photon and d_{eg} the dipole matrix element between the ground and excited states. For atoms spaced at distances small compared to the optical wavelength, retardation effects are negligible, and the level shift arising from the near field dipole-dipole interaction scales as $V_{dd} \sim \langle d_1 \rangle \langle d_2 \rangle / r_{12}^3$, where $\langle d \rangle$ is the dipole expectation value and r_{12} is the characteristic separation between the dipoles. For weak (nonsaturated) excitation, $\langle d \rangle \sim \sqrt{s} d_{eg}$, which means that the ratio of interaction energy to scattering rate scales as

$$\kappa \sim \frac{V_{dd}}{\hbar \Gamma'} \sim (kr_{12})^{-3}. \quad (1)$$

Thus, if the atoms can be tightly confined to relative distances small compared to the wavelength, one can induce a coherent dipole-dipole interaction with negligible photon scattering. The key feature is that while the coherent level shift can be enhanced substantially through tight confinement, the cooperative spontaneous emission rate cannot be enhanced by more than a factor of two (the Dicke superradiant state) over that of an isolated atom.

We propose here a new system for implementing quantum logic gates: neutral atoms trapped in a far-off-resonance optical lattice and interacting via induced coherent dipole-dipole

interactions. Optical lattices are periodic potentials created by a set of interfering laser beams in which atoms are trapped via the ac-Stark shift [16]. By detuning the lasers very far from resonance, photon scattering is almost completely suppressed, while high intensities maintain substantial potential wells. Through a combination of near-resonance Sisyphus laser cooling and adiabatic transfer to a far-off-resonance lattice [17], combined with resolved sideband Raman cooling [18], atoms can be prepared in the ground state of the potential wells. For example, in a recent experiment, $\sim 10^6$ Cs atoms were cooled nearly to the vibrational ground state in a two-dimensional optical lattice, with mean vibrational excitation $\bar{n} \approx 0.01$ [18]. Atoms so trapped are tightly confined, with an rms spread on the order of $\Delta x \approx \lambda / 50$ for reasonably deep wells, and are thus good candidates for inducing coherent dipole-dipole interactions. According to Eq. (1), the ratio of the level shift to the linewidth is $\kappa = C / \eta^3 \approx 500 C$, where $\eta = k\Delta x$ is the Lamb-Dicke parameter, and C is a number depending on the details of the geometry. Such a figure of merit is very promising for implementing quantum logic. In addition, optical lattices are an especially promising candidate for scaling quantum computation to operate with many qubits, since cooling, preparing, and manipulating the atoms can be performed in parallel on a large ensemble of noninteracting atoms.

Consider the three-dimensional optical lattice shown in Fig. 1. The “transverse” beams have frequency ω_T , detuned very far to the blue of the atomic resonance, and propagating in the x - y plane with polarization along z . They form a two dimensional π -polarized standing wave, which confines the atoms in tubes at its nodes arranged in a square array of periodicity $\lambda_T/2$. The “longitudinal” confining beams have frequency ω_L , detuned very far to the red, producing standing waves of σ_+ and σ_- light that form a one dimensional optical lattice with the familiar antiferromagnetic order [16]. By choosing the longitudinal and transverse fields with frequencies that differ by many atomic linewidths, but far from any Raman resonance, we can treat the two fields independently, with no interference terms. Near the minima of the wells, the potentials can be approximated as harmonic, with curvature determined by the laser

intensity and by the Clebsch-Gordan coefficients for the particular transitions driven by the fields. Through an appropriate choice of laser intensities and detunings, we can make the potential axially symmetric. Such ellipsoidal potential wells maximize the dipole-dipole interaction, as we show below.

Central to our method is the ability to vary the lattice geometry dynamically. The antiferromagnetic order of the atoms tightly trapped by longitudinal fields allows the distinction of two “species” of atoms: those that reside in σ_+ -polarized wells and those that reside in σ_- -polarized wells. Changing the angle between the longitudinal lasers’ polarizations varies the distance δZ between the minima of these wells according to $k_L(\delta Z) = \tan^{-1}(\tan \theta / 2)$ (see Fig. 1). Two atoms trapped in neighboring wells can be brought into the same linearly polarized well by rotating the lasers’ polarization to parallel, adiabatically compared with the oscillation frequency in the well. We take the lattice lasers to have large detunings compared to any hyperfine splitting in the D2 resonance ($S_{1/2} \rightarrow P_{3/2}$), but small compared to the fine-structure splitting. In that case the nuclear spin becomes essentially irrelevant, and the light shift is effectively that of a $J_g = 1/2 \rightarrow J_e = 3/2$ transition, with no coherences $\Delta M_F = \pm 2$ [20]. Thus, as the lasers’ polarizations are rotated, there is no possibility of causing electronic transitions via stimulated $\sigma_+ - \sigma_-$ Raman transitions. When the longitudinal laser field is linearly polarized, all of the sublevels see the same light shift potentials.

Once in the same well, the atoms can be made to interact by applying an auxiliary “catalysis laser” tuned closer to resonance, which excites the atomic dipoles for a short time. In this way the atoms interact *only* during the two-bit logical operations. Afterwards, the atoms can be separated by further adiabatic rotation of the laser polarizations. Note that a rotation of the laser polarization beyond 90° slides the potential wells by more than a quarter wavelength; atoms initially spaced n wells apart can be brought together by a continuous rotation of one beam’s polarization by $n\pi/2$ rad. In principle any two atoms of opposite

species within a tube can be brought into the same potential well, thereby creating the possibility of entangling large numbers of atoms via a sequence of two-qubit operations.

As an example of quantum logic within our scheme, consider alkalis trapped in the lattice described above. For each of the σ_{\pm} atomic “species”, we define a computational basis, $|1\rangle_{\pm}, |0\rangle_{\pm}$, of logical one and zero,

$$|1\rangle_{+} \equiv |F_{\uparrow}, M_F = 1\rangle \otimes |n = 0\rangle, \quad |0\rangle_{+} \equiv |F_{\downarrow}, M_F = -1\rangle \otimes |n = 0\rangle,$$

$$|1\rangle_{-} \equiv |F_{\uparrow}, M_F = -1\rangle \otimes |n = 0\rangle, \quad |0\rangle_{-} \equiv |F_{\downarrow}, M_F = 1\rangle \otimes |n = 0\rangle,$$

where $F_{\uparrow,\downarrow} = I \pm 1/2$ are the two hyperfine levels associated with the $S_{1/2}$ ground state and nuclear spin I (half-integer), M_F is the magnetic sublevel, and $|n = 0\rangle$ is the vibrational ground state of the associated potential. Single-qubit operations can be performed via $\sigma_{+}-\sigma_{-}$ pulses that are Raman-resonant with one species of atom, but are detuned far from the excited state manifold. These single-qubit manipulations can be applied in parallel to the entire ensemble of a given species if an external magnetic field is also used. This ensures that the pulses do not transfer population of the other atomic species out of the computational basis.

Two-qubit operations involve conditioning the state of one atom on the state of the other. For example a C-NOT can be performed in the following way. Two atoms are made to reside in the same well as described above, and an auxiliary laser is used to excite a near-resonant atomic dipole. We take this catalysis field to be a traveling wave, polarized along the z -axis. The probability of spontaneous emission and radiation pressure, both of which scale linearly with s , are negligible for small intensities. If the catalysis laser is detuned near the $|S_{1/2}, F_{\uparrow}\rangle \rightarrow |P_{3/2}, F'_{\max}\rangle$ transition, where $F'_{\max} = I + 3/2$, but with a detuning small compared to the ground state hyperfine splitting, a dipole is excited only if the atom is in the $|F_{\uparrow}\rangle$ state (i.e., the logical states $|1\rangle_{\pm}$). Thus the dipole-dipole interaction causes a shift only of the $|1\rangle_{-} \otimes |1\rangle_{+}$ two-qubit state and has neither diagonal nor off-diagonal matrix elements between any of the other two-qubit registers. For example, suppose the σ_{-} species

acts as the control bit and the σ_+ acts as the target. A $\sigma_+ - \sigma_-$ Raman π -pulse on the shifted $|1\rangle_- \otimes |1\rangle_+ \leftrightarrow |1\rangle_- \otimes |0\rangle_+$ transition achieves a C-NOT with the usual truth table. The polarizations of the Raman lasers and an external magnetic field ensure that the pulse is not resonant with any other transition (see Fig. 2).

One could also perform a “controlled-phase gate” without an external Raman pulse. If the atoms freely evolve in a common well while in the presence of the catalysis laser for a time $\tau = \hbar\pi / \langle V_{dd} \rangle$, then only the $|1\rangle_+ \otimes |1\rangle_-$ state experiences a change in sign. This gate together with single bit rotations is universal to quantum logic [21], and has the advantage of not requiring any mechanism for distinguishing $|0\rangle_- \otimes |1\rangle_+$ from $|1\rangle_- \otimes |0\rangle_+$.

The complete dipole-dipole interaction is dependent both on the internal electronic states of the atoms, which determine the tensor nature of the dipole, and on the external motional states, which determine the atomic wave function overlap with the dipole-dipole potential. In the low saturation limit, the excited states can be adiabatically eliminated and the dipole-dipole interaction Hamiltonian between a pair of atoms can be written as [21]

$$H_{dd} = V_{dd} - i\Gamma_{dd} = -\frac{\hbar\Gamma'}{2} \left[\left(\mathbf{D}_2 \cdot \vec{\varepsilon}_c \right)^\dagger \left\{ \mathbf{D}_1 \cdot \left(\vec{\mathbf{f}}(\mathbf{r}_{12}) + i\vec{\mathbf{g}}(\mathbf{r}_{12}) \right) \cdot \mathbf{D}_2^\dagger \right\} \left(\mathbf{D}_1 \cdot \vec{\varepsilon}_c \right) + H.c. \right].$$

The Hermitian part V_{dd} describes the level shift whereas Γ_{dd} describes the enhancement of the spontaneous photon scattering rate due to cooperative effects. The scaled dipole operator for atom i is defined by $\mathbf{D}_i = P_e \mathbf{d}_i P_g / \langle e \| d_i \| g \rangle$, where $\langle e \| d_i \| g \rangle$ is the reduced matrix element, and $P_{e,g}$ are projectors on the ground and excited manifolds. The scattering rate Γ' is determined by the intensity and detuning of the catalysis laser, which has polarization $\vec{\varepsilon}_c$, and an atomic transition with unit Clebsch-Gordan coefficient; we assume here that only one excited state manifold participates in the excitation. The c-number tensors $\vec{\mathbf{f}}$ and $\vec{\mathbf{g}}$ describe the dependence of the dipole-dipole interaction on the relative position of the two atoms. For small distances $\vec{\mathbf{f}}(\mathbf{r}_{12})$ scales as $1/r_{12}^3$ whereas $\vec{\mathbf{g}}(\mathbf{r}_{12})$ goes to unity, corresponding to the full cooperativity of the superradiant state.

For vector dipoles induced by the π -polarized catalysis laser and ignoring energy non-conserving processes that take the atoms out of the computational basis via virtual photon exchanges, H_{dd} is diagonal in the computational subspace, with the only nonvanishing matrix element given by

$$\langle 1_+, 1_- | H_{dd} | 1_+, 1_- \rangle = -\hbar\Gamma' c_g^4 \langle f_{00}(r, \theta_r) + ig_{00}(r, \theta_r) \rangle,$$

$$f_{00}(r, \theta_r) + ig_{00}(r, \theta_r) = ih_0^{(2)}(k_c r) + P_2(\cos \theta_r) ih_2^{(2)}(k_c r).$$

Here c_g is the Clebsch-Gordan coefficient for the dipole transition $|F_\uparrow, M_F = \pm 1\rangle \rightarrow |F'_{\max}, M_{F'} = \pm 1\rangle$, $h_{0,2}^{(2)}(x) = j_{0,2}(x) - i n_{0,2}(x)$ are spherical Hankel functions, and $P_2(\mu)$ is the second-order Legendre polynomial. The figure of merit is then given by

$$\kappa \equiv \frac{\langle V_{dd} \rangle}{\langle \hbar(c_g^4 \Gamma' + \Gamma_{dd}) \rangle} = \frac{-\langle f_{00}(r, \theta_r) \rangle}{1 + \langle g_{00}(r, \theta_r) \rangle}.$$

The expectation value over the external coordinates is taken with respect to the relative coordinate probability density for the two atoms, having traced over the center of mass. Though spherically symmetric wells maximize the radial wave function overlap for atoms in their ground vibrational states, the relative coordinate wave function is proportional to Y_0^0 , which is orthogonal to the Y_2^0 potential. One solution is to make use of ellipsoidal wells which maximize both the radial confinement and the overlap with the angular distribution of the multipole.

Consider an axially symmetric harmonic potential with two atoms in the vibrational ground state, each described by a Gaussian wave packet with widths $\Delta x = \Delta y \equiv x_0$ and $\Delta z \equiv z_0$. Fig. 3 shows a plot of κ , calculated numerically, as a function $\eta_x = kx_0$ and $\eta_z = kz_0$. Over the range of values shown, $\langle g_{00}(r, \theta_r) \rangle \approx 1$, i.e. full cooperativity. For example, given experimentally accessible localizations $x_0 = \lambda / 60$ and $z_0 = \lambda / 30$,

corresponding to $\eta_x \approx 0.1$ and $\eta_z \approx 0.2$, the figure of merit is $\kappa \approx -19.3$. This is sufficient to clearly resolve the levels as shown in Fig. 2.

In order to optimize the figure of merit, we consider an approximate analytic expression for κ for tight localization. Taking only the near field contribution to H_{dd} , we have

$$\kappa \approx \frac{3\hbar\Gamma'}{8\sqrt{\pi}\eta_x^2\eta_z} \int_0^\infty \frac{dr}{r} \int_{-1}^1 d(\cos\theta) P_2(\cos\theta) \exp\left\{-\left(\frac{\sin^2\theta}{4x_0^2} - \frac{\cos^2\theta}{4z_0^2}\right)r^2\right\}. \quad (2)$$

Though this integral appears to have a logarithmic divergence at $r = 0$, this is not the case since the angular integration goes like r^2 for small r [22]. It is also clear from Eq.(2) that the dipole-dipole level shift vanishes for spherical wells due to the orthogonality of the Legendre polynomials. We can evaluate this expression by making the radial integral converge through the substitution $1/r \rightarrow 1/r^{(1+\varepsilon)}$. After taking the limit $\varepsilon \rightarrow 0$ we find

$$\kappa \approx \frac{1}{8\sqrt{\pi}\eta_x^2\eta_z} \left[-2 - 3\frac{\eta^2}{\eta_x^2} + 3\left(\frac{\eta^3}{\eta_x^3} + \frac{\eta}{\eta_x}\right) \tan^{-1}\left(\frac{\eta_x}{\eta}\right) \right], \text{ where } \frac{1}{\eta^2} \equiv \frac{1}{\eta_z^2} - \frac{1}{\eta_x^2}.$$

Assuming a best achievable localization in any dimension, it is clearly advantageous to choose $x_0 < z_0$. Keeping η_x fixed, we can then maximize κ with respect to the ratio η_z / η_x , with the result $(\eta_z / \eta_x)_{\max} \approx 2.18$, giving $\kappa_{\max} \approx -0.017 / \eta_x^3$. The relatively small prefactor can be attributed to two contributions: the rms width of the relative coordinate Gaussian wave function in three dimensions is at least $\sqrt{6}$ times the rms for a single particle in 1D, and the overlap of the angular distribution of the dipoles and $P_2(\cos\theta)$ is imperfect. Nonetheless, the enhancement arising from the tight confinement is sufficient to obtain a resolvable level shift.

Though optical lattices hold promise for producing entangled states of a few atoms, much remains to be done to implement even a rudimentary quantum computation. From the experimental side, the filling fraction of atoms in the lattice must be increased over its current value of $\sim 1\%$. Work in this direction is currently underway. The Berkeley group has

achieved densities of $\sim 10^{12}$ cm $^{-3}$ in the type of lattice described here, corresponding to a filling fraction $\sim 10\%$ [23]. In addition, one must develop a method for addressing and reading out the state of individual qubits. One possibility is to design lattices with more widely separated wells through the superposition of many different wave vectors or the use of very long wavelength lasers (such as an intense CO₂ laser [24]). The difficulty here is to maintain tight confinement of the atoms. Alternatively, one could employ tomography to tag the atomic resonance to the position of a well by use of a gradient magnetic field or an additional ac Stark shift [25]. A major theoretical issue is the effect of atomic collisions [26]. Even for atoms in the ground state, long range molecular potentials can play an important role in atom-atom interactions for densities corresponding to two atoms in the same well. Though such interactions might be destructive for atoms in the excited state [27], elastic collisions might actually be useful to improve the figure of merit by providing level shifts with a lower decoherence rate [28]. Another important question is that of error correction. For example, in our scheme, each one dimensional “tube” of atoms constitutes a separate quantum register acting in parallel with all the others; one might capitalize on this massive parallelism to increase the error threshold for fault tolerant computation. Optical lattices are extremely flexible, with many experimental “knobs”, allowing a wide variety of possible mechanisms for implementing the essential features of quantum logic.

Acknowledgments: We would like to thank Paul Alsing and John Grondalski for many useful discussions. This work was supported in part by New Mexico Universities Collaborative Research (Grant No. 9769). CMC acknowledges support from the Office of Naval Research (Grant No. N00014-93-1-0116). PSJ was supported by the National Science Foundation (Grant No. PHY-9503259), by the Army Research Office (Grant No. DAAG559710165), and by the Joint Services Optics Program (Grant No. DAAG559710116).

References

- [1] D. P. DiVincenzo, *Science* **270**, 255 (1995); A. Ekert and R. Jozsa, *Rev. Mod. Phys.* **68**, 733 (1996).
- [2] P. W. Shor, *Phys. Rev. A* **52**, 2493 (1995).
- [3] A. Ekert and C. Macchiavello, *Phys. Rev. Lett.* **77**, 2585 (1996).
- [4] E. Knill and R. Laflamme, *Phys. Rev. A* **55**, 900 (1997).
- [5] A. R. Caldebank et al. *Phys. Rev. Lett.* **78**, 405 (1997).
- [6] D. Gottesman, *Phys. Rev. A* **54**, 1862 (1996).
- [7] J. Preskill, *Proc. Roy. Soc. A*, **454** 385 (1998).
- [8] E. Knill, R. Laflamme, and W. Zurek, *Science* **279**, 342 (1998).
- [9] J. I. Cirac and P. Zoller, *Phys. Rev. Lett.* **74**, 4094 (1995).
- [10] C. Monroe et. al *Phys. Rev. Lett.* **75**, 4714 (1995).
- [11] D. Wineland et. al, *J. Res. Natl. Inst. Stand. Tech.* (1998).
- [12] N. A. Gershenfeld and I. L. Chuang, *Science* **275**, 350 (1997).
- [13] P. Domokos, et al., *Phys. Rev. A* **52**, 3554 (1995); Q. A. Turchette et al., *Phys. Rev. Lett.* **75**, 4710 (1995).
- [15] A. Barenco et al., *Phys. Rev. Lett.* **74**, 4083 (1995)
- [16] For a review of optical lattices see, P. S. Jessen and I. H. Deutsch, *Adv. Atom. Mol. Opt. Phys.* **36**, 91 (1996), and references therein.
- [17] D. L. Haycock et al., *Phys. Rev. A* **55**, R3991 (1997).
- [18] S. E. Hamann et al., *Phys. Rev. Lett.* **80**, 4149 (1998).
- [19] I. H. Deutsch and P. S. Jessen, *Phys. Rev A* **57**, 1972 (1998).
- [20] A. Barenco et al., *Phys. Rev. A* **52**, 3457 (1995).
- [21] E.V. Goldstein, P. Pax, and P. Meystre, *Phys. Rev. A* , **53**, 2604 (1996). J. Gou and J. Cooper, *Phys. Rev. A* **51**, 3128 (1995).
- [22] M.G. Moore and P. Meystre, *Phys. Rev A* **56**, 2989 (1997).

- [23] D. Weiss (private communication).
- [24] S. Friebel et al., Phys Rev A **57** R20 (1998).
- [25] J.R. Gardner et al., Phys. Rev. Lett. **70** 3404 (1993).
- [26] P. S. Julienne and F. H. Mies, J. Opt. Soc. Am. B **6**, 2257 (1989).
- [27] C. Boisseau and J Vigu , Opt. Comm. **127**, 251 (1996).
- [28] J. L. Bohn and P. S. Julienne, Phys. Rev. A. **56**, 1486 (1997).

Figure Captions

Fig 1. Schematic of a 3D optical lattice. Two pairs of π -polarized beams k_T , detuned very blue of resonance, provide transverse confinement, and the beams k_L , detuned very red, provide longitudinal confinement in σ_+ and σ_- standing waves. The solid (dotted) contours represent the resulting ellipsoidal potential wells associated the σ_+ (σ_-) polarization, separated pairwise by δZ , as a function of the relative polarization angle θ .

Fig 2. Schematic energy levels for the D2 line of a generic alkali in the presence of a small longitudinal magnetic field (not to scale). The computational basis states for atoms that follow σ_{\pm} light are indicated. The catalysis laser ω_c is near resonant and blue detuned for $|1\rangle_{\pm}$ states. The transverse and longitudinal trapping frequencies ω_T, ω_L are detuned very far from resonance. Unitary manipulation via a Raman pulse connecting only the $|0\rangle_+$ and $|1\rangle_+$ states is shown.

Fig. 3. Plot of κ , the ratio of the coherent dipole-dipole level shift to the total incoherent linewidth, as a function of the Lamb-Dicke localization parameter in the transverse direction, η_x , and the longitudinal direction, η_z .

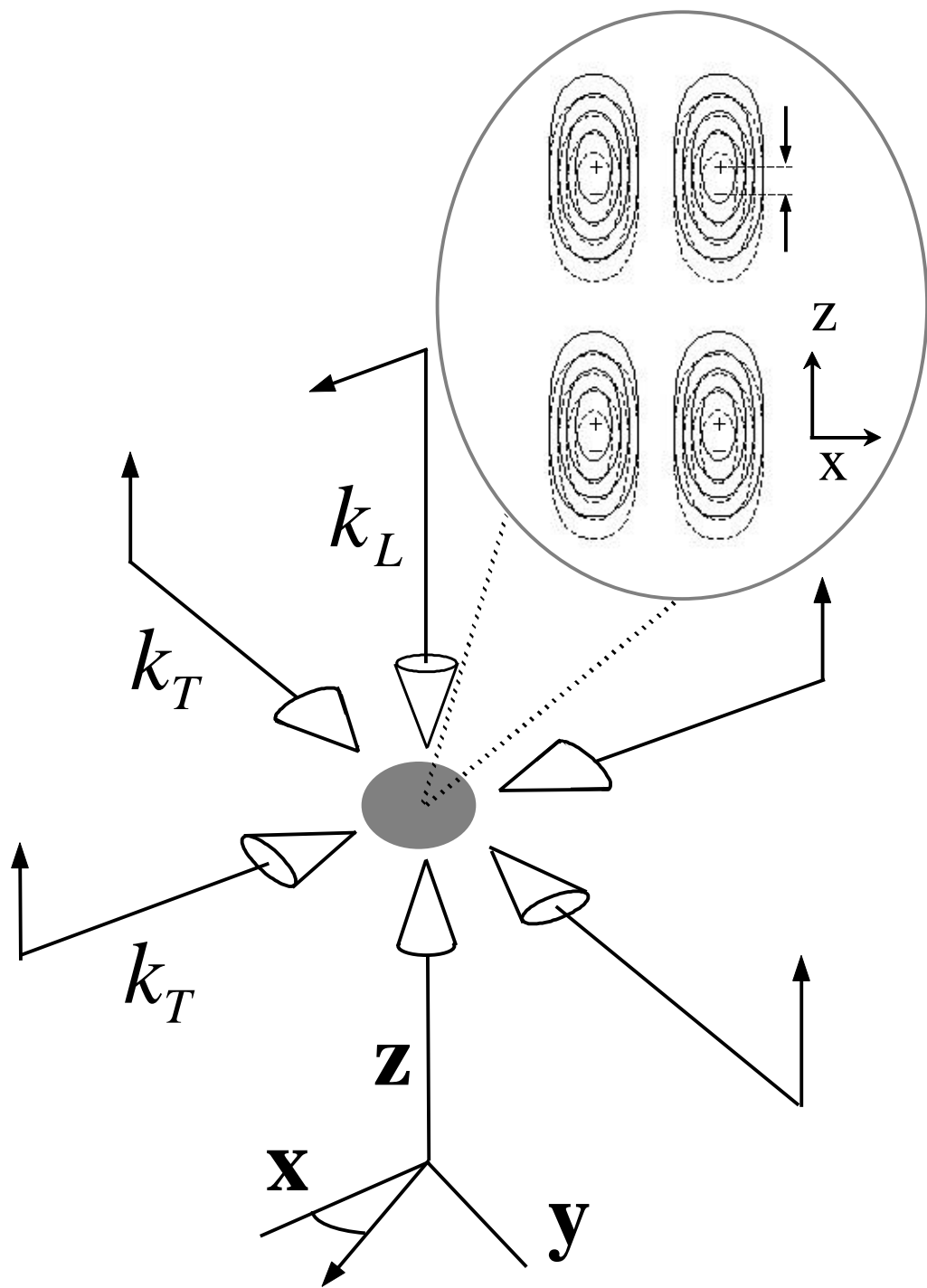


Fig. 1

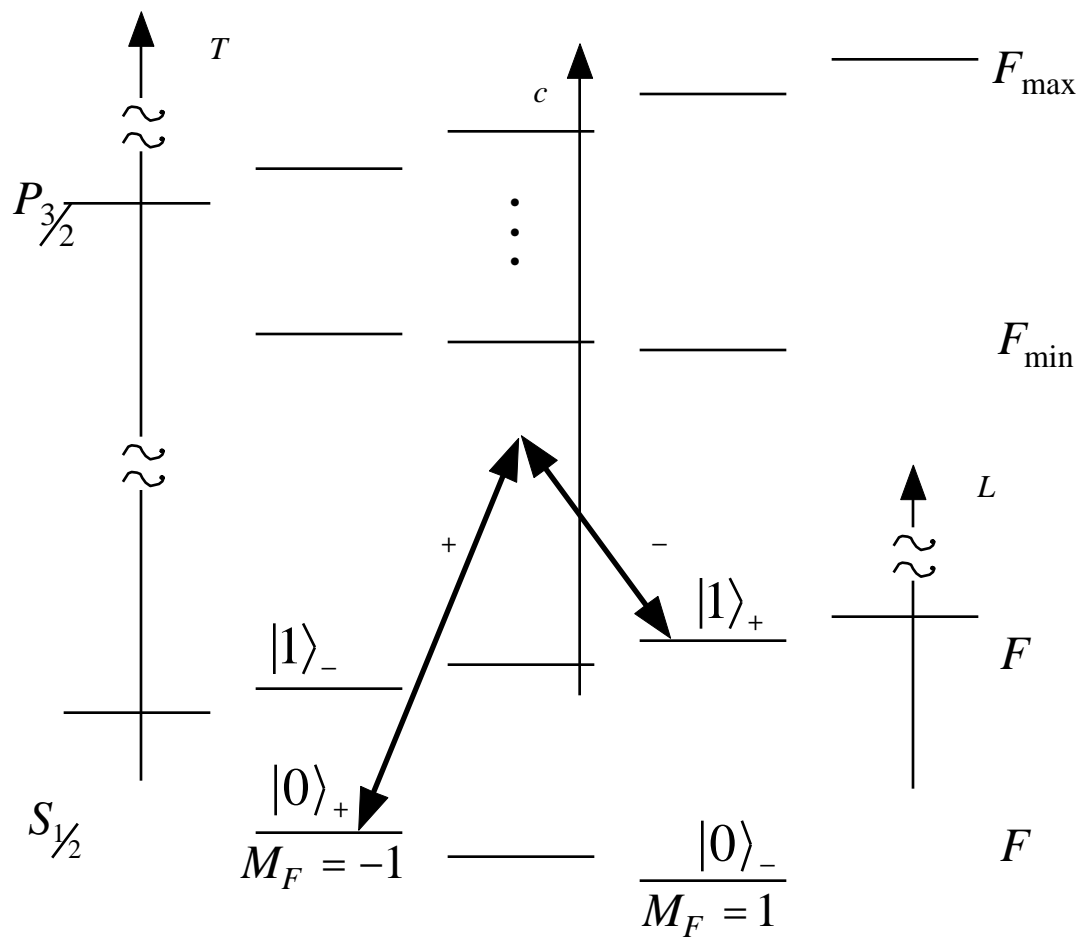


Fig. 2

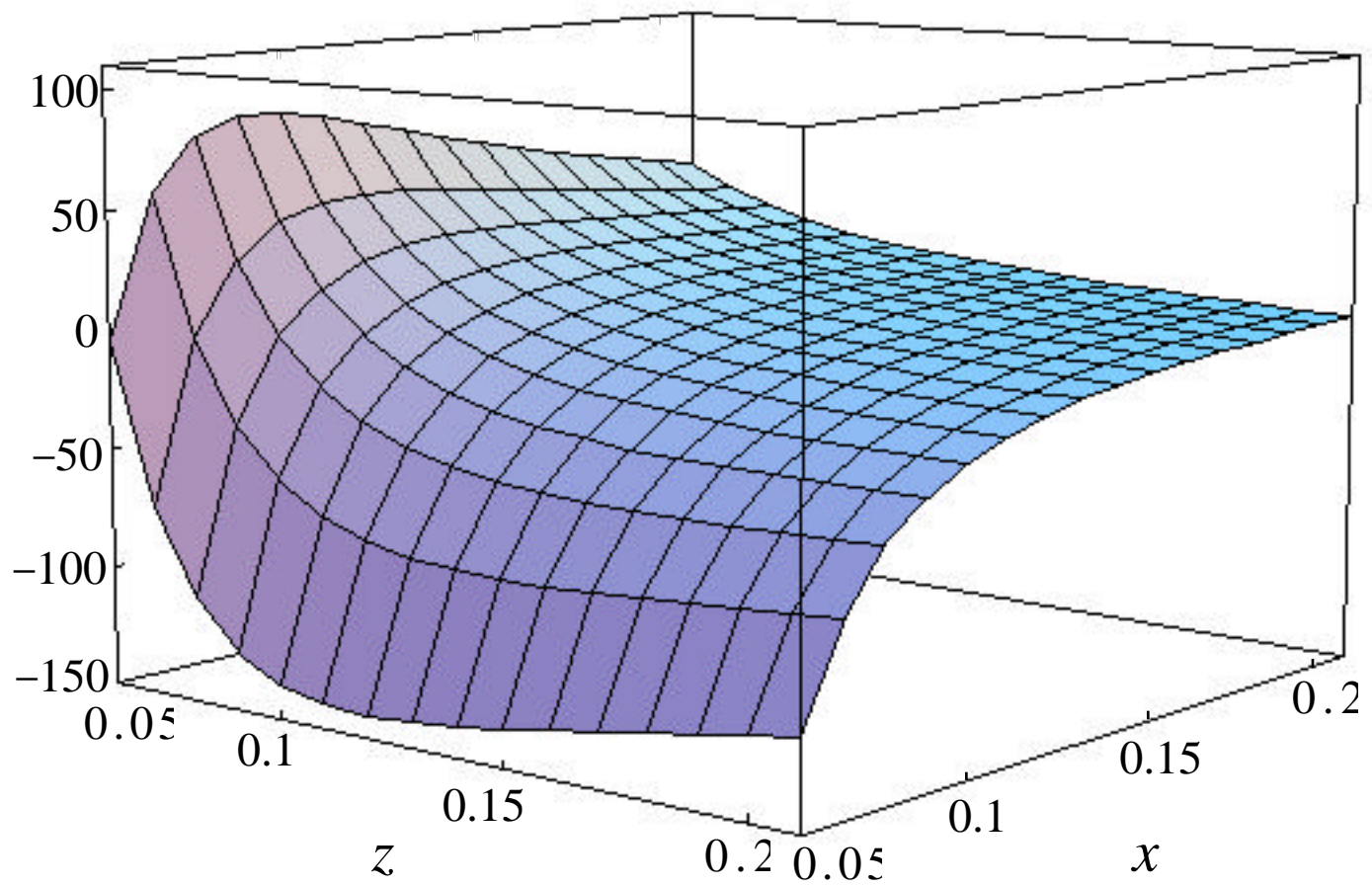


Fig. 3